Available online at www.sciencedirect.com
SCIENCE DIRECT®
Solar Energy Materials & Solar Cells
ELSEVIER
Solar Energy Materials & Solar Cells 80 (2003) 1–20
www.elsevier.com/locate/solmat

Highly stable amorphous silicon hydride

Randell L. Mills*, Bala Dhandapani, Jiliang He

BlackLight Power, Inc. 493 Old Trenton Road, Cranbury, NJ 08512, USA

Received 10 February 2003

Abstract

A novel highly stable hydrogen terminated silicon coating was synthesized by microwave plasma reaction of mixture of silane, hydrogen, and helium wherein it is proposed that He^+ served as a catalyst with atomic hydrogen to form highly stable silicon hydrides. Novel silicon hydride was identified by time of flight secondary ion mass spectroscopy (ToF-SIMS) and X-ray photoelectron spectroscopy (XPS). The ToF-SIMS identified the coatings as hydride by the large SiH^+ peak in the positive spectrum and the dominant H^- in the negative spectrum. Since hydrogen is the only element with no primary element peaks, XPS identified the H content of the SiH coatings as comprising novel silicon hydrides due to new peaks at 11, 43, and 55 eV in the absence of corresponding peaks of any candidate element at higher binding energies. The silicon hydride surface was remarkably stable to air as shown by XPS. The highly stable amorphous silicon hydride coating may advance the production of integrated circuits and microdevices by resisting the oxygen passivation of the surface and possibly altering the dielectric constant and band gap to increase device performance.
© 2003 Elsevier B.V. All rights reserved.

1. Introduction

Aqueous HF acid etching of silicon surfaces results in the removal of the surface oxide and produces hydrogen terminated silicon surfaces, Si–H. HF etching is a key step in producing silicon surfaces which are contamination-free and chemically stable for subsequent processing in the semiconductor industry [1–3]. In fact, chemical oxidation and subsequent HF treatment of Si surfaces are used prior to gate oxidation, where surface contamination (<10 ppm level) and interface control are crucial to device performance. Fluorine termination was initially considered the

*Corresponding author. Tel.: +1-609-490-1090; fax: +1-609-490-1066.
E-mail address: rmills@blacklightpower.com (R.L. Mills).

0927-0248/03/$ - see front matter © 2003 Elsevier B.V. All rights reserved.
doi:10.1016/S0927-0248(03)00107-7

basis of the chemical stability of HF-treated surfaces. Subsequently, it was found that fluorine is a minor species on the surface and that the remarkable surface passivation achieved by HF is explained by H termination of silicon dangling bonds protecting the surface from chemical attack [3–5]. However, the replacement of the oxide layer with the H termination of the silicon dangling bonds by HF can be attributed to the increased electronegativity of fluoride ion versus oxide causing an enhanced reactivity of H^+ which attacks the oxide layer. The electron affinity of halogens increases from the bottom of the Group VII elements to the top. Hydride ion may be considered a halide since it possess the same electronic structure. And, according to the binding energy trend, it should have a high binding energy. However, the binding energy is only 0.75 eV which is much lower than the 3.4 eV binding energy of a fluoride ion. And, once the HF is rinsed from the surface, the Si–H layer undergoes rapid oxidation when exposed to oxygen or solvents containing oxygen. An Si–H layer with enhanced stability would be of great value to the semiconductor industry.

Amorphous Si–H films, the active component of important semiconductor devices such as photovoltaics, optoelectronics, liquid crystal displays, and field-effect transistors are formed by plasma enhanced chemical vapor deposition (PECVD) techniques [6]. A review of the current state of photovoltaic technology is given by Green [7]. Typically the film is grown on a silicon wafer substrate exposed to a plasma of silane, hydrogen, and often argon using a reactor with a diode configuration in which the plasma is confined between two parallel electrodes. In this study, we find that the aqueous HF acid etched surface undergoes rapid oxidation when exposed to air and provides little protection from such exposure. Whereas, a novel highly air stable amorphous silicon hydride surface coating designated α-SiH was synthesized by microwave plasma reaction of mixture of silane, hydrogen, and helium wherein it is proposed that He^+ served as a catalyst with atomic hydrogen. The novel α-SiH film may advance semiconductor fabrication and devices.

It was reported previously that a new plasma source has been developed that operates by incandescently heating a hydrogen dissociator to provide atomic hydrogen and heats a catalyst such that it becomes gaseous and reacts with the atomic hydrogen to produce a plasma called a resonant transfer or rt-plasma. It was extraordinary, that intense VUV emission was observed [8] at low temperatures (e.g. $\approx 10^3$ K) and an extraordinary low field strength of about 1–2 V/cm from atomic hydrogen and certain atomized elements or certain gaseous ions which singly or multiply ionize at integer multiples of the potential energy of atomic hydrogen, 27.2 eV. In this study, He^+ was used as a catalyst to form α-SiH since the second ionization energy of helium is 54.417 eV, which is equivalent to $2 \cdot 27.2$ eV. In this case, 54.417 eV is transferred nonradiatively from atomic hydrogen to He^+ which is resonantly ionized. The catalysis reaction products are highly stable intermediates which react to form novel stable hydrides. Hydride ions with high binding energies have been observed by X-ray photoelectron spectroscopy (XPS) and by solid state magic-angle spinning proton nuclear magnetic resonance (^{1}H MAS NMR) having upfield shifted peaks [9]. Additional prior related studies that support the possibility

of a novel reaction of atomic hydrogen which produces a chemically generated or assisted plasma (rt-plasma) and produces novel hydride compounds include extreme ultraviolet (EUV) spectroscopy [8,10–26], characteristic emission from catalysts and the hydride ion products [14–17], lower-energy hydrogen emission [10–12,18,19,24,25], chemically formed plasmas [8,13–17,20,21], Balmer α line broadening [8,11,12,14,22–25,27], inverted hydrogen populations [26], anomalous plasma afterglow duration [20,21], power generation [11,12,23–25], and analysis of novel chemical compounds [28–31]. The theory was given previously [10–12].

Even a partial coating of an extremely stable silicon hydride may stabilize a silicon surface to unprecedented time scales to increase the yield in integrated chip fabrication. In this paper, we report the results of the reaction of silane in a helium–hydrogen microwave discharge plasma at the surface of a nickel foil. After the plasma reaction processing, the surface was characterized by ToF-SIMS and XPS.

2. Experimental

2.1. Synthesis

Amorphous silicon hydride (α-SiH) films were grown on nickel substrates by their exposure to a low pressure microwave discharge of SiH_4 (2.5%)/He (96.6%)/H_2 (0.9%). The experimental set up comprising a microwave discharge cell operated

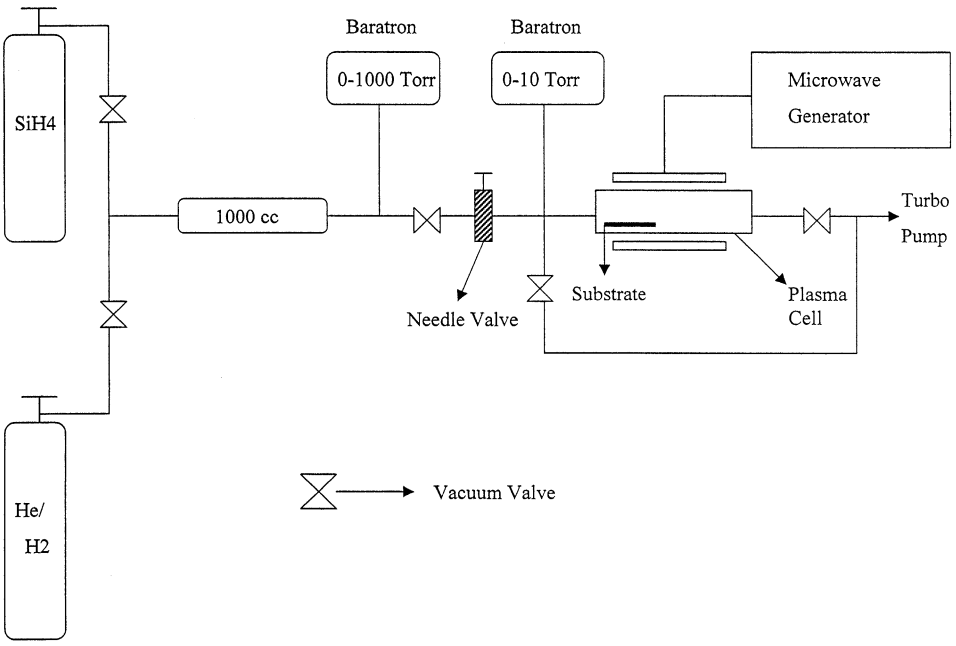

Fig. 1. The experimental set up comprising a microwave discharge cell operated under flow conditions.

under flow conditions is shown in Fig. 1. The SiH_4 gas was introduced into a 1000 ml reservoir by a gas/vacuum line where it was mixed with premixed He (99%)/H_2 (1%) to obtain the reaction mixture SiH_4 (2.5%)/He (96.6%)/H_2 (0.9%) by controlling the individual gas pressures. Nickel foil (5×5 and 0.05 mm thick, Alfa Aesar 99 + %) substrates were used instead of silicon wafers to avoid charging during time of flight secondary ion mass spectroscopy (ToF-SIMS) and XPS characterization as well background interference in the analysis. The substrates were placed inside of a quartz tube (1.3 cm in diameter by 15.5 cm long) with vacuum valves at both ends. The tube was fitted with an Opthos coaxial microwave cavity (Evenson cavity) and connected to the gas/vacuum line. The quartz tube and vacuum line were evacuated sufficiently to remove any trace moisture or oxygen. The gas mixture SiH_4 (2.5%)/He (96.6%)/H_2 (0.9%) was flowed through the quartz tube at a total pressure of 0.7 Torr maintained with a gas flow rate of 40 sccm controlled by a mass flow controller with a readout. The cell pressure was monitored by an absolute pressure gauge. The microwave generator shown in Fig. 1 was an Opthos model MPG-4M generator (Frequency: 2450 MHz). The microwave plasma was maintained with a 40 W (forward)/15 W (reflected) power for about 20 min. Yellow-orange coatings formed on the substrates and the wall of the quartz tube. The quartz tube was removed and transferred to a drybox with the samples inside by closing the vacuum valves at both ends and detaching the tube from the vacuum/gas line. The coated substrates were mounted on XPS and ToF-SIMS sample holders under an argon atmosphere in order to prepare samples for the corresponding analyses. One set of samples was analyzed with air exposure limited to 10 min and another for 20 min while transferring and mounting during the analyses. Separate samples were removed from the drybox and stored in air at room temperature for 48 h or 10 days before the analyses. Controls comprised a commercial silicon wafer (Alfa Aesar 99.99%) untreated, and HF cleaned silicon wafers exposed to air for 10 min or 3 h.

2.2. ToF-SIMS characterization

The commercial silicon wafer, HF cleaned silicon wafer, and α-SiH coated nickel foil samples were characterized using Physical Electronics TRIFT ToF-SIMS instrument. The primary ion source was a pulsed $^{69}Ga^+$ liquid metal source operated at 15 keV [32] (for recent specifications see [33]). The secondary ions were exacted by a ± 3 keV (according to the mode) voltage. Three electrostatic analyzers (triple-focusing-time-of-flight) deflect them in order to compensate for the initial energy dispersion of ions of the same mass. The 400 pA DC current was pulsed at a 5 kHz repetition rate with a 7 ns pulse width. The analyzed area was $60 \times 60\ \mu m^2$ and the mass range was 0–1000 AMU. The total ion dose was 7×10^{11} ions/cm^2, ensuring static conditions. Charge compensation was performed with a pulsed electron gun operated at 20 eV electron energy. In order to remove surface contaminants and expose a fresh surface for analysis, the samples were sputter-cleaned for 30 s using a $80 \times 80\ \mu m^2$ raster, with 600 pA current, resulting in a total ion dose of 10^{15} ions/cm^2. Three different regions on each sample of $60 \times 60\ \mu m^2$ were analyzed. The positive and negative SIMS spectra were acquired. Representative post-sputtering data is

reported. The ToF-SIMS data were treated using 'Cadence' software (Physical Electronics), which calculates the mass calibration from well-defined reference peaks.

2.3. XPS characterization

A series of XPS analyses were made on the samples using a Scienta 300 XPS Spectrometer. The fixed analyzer transmission mode and the sweep acquisition mode were used. The angle was 15°. The step energy in the survey scan was 0.5 eV, and the step energy in the high-resolution scan was 0.15 eV. In the survey scan, the time per step was 0.4 s, and the number of sweeps was 4. In the high-resolution scan, the time per step was 0.3 s, and the number of sweeps was 30. C 1s at 284.5 eV was used as the internal standard.

3. Results and discussion

3.1. ToF-SIMS

The positive ToF-SIMS spectra ($m/e = 0-100$) of the noncoated cleaned commercial silicon wafer and a nickel foil coated with an α-SiH film and exposed to air for 10 min are shown in Figs. 2 and 3, respectively. The positive ion spectrum of the control was dominated by Si^+, oxides $Si_xO_y^+$, and hydroxides $Si_x(OH)_y^+$; whereas, that of the α-SiH sample contained essentially no oxide or hydroxide peaks. Rather, it was dominated by Si^+ and a peak at $m/z = 29$ which comprised a contribution from SiH^+ and $^{29}Si^+$ which were difficult to separate definitively.

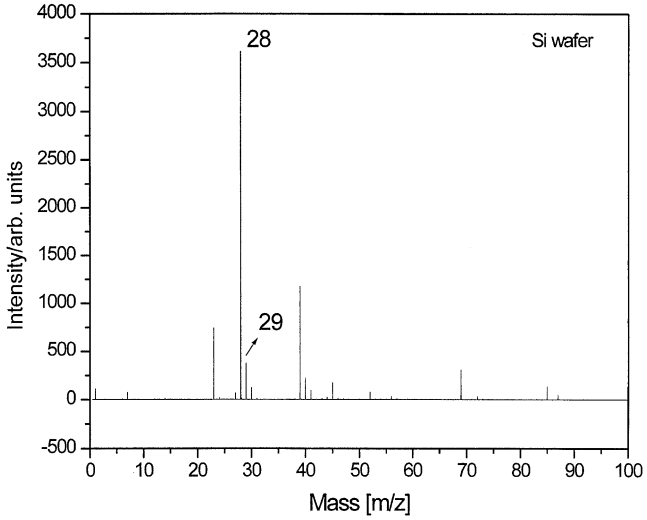

Fig. 2. The positive ion ToF-SIMS spectra ($m/e = 0-100$) of a noncoated cleaned commercial silicon wafer (Alfa Aesar 99.9%).

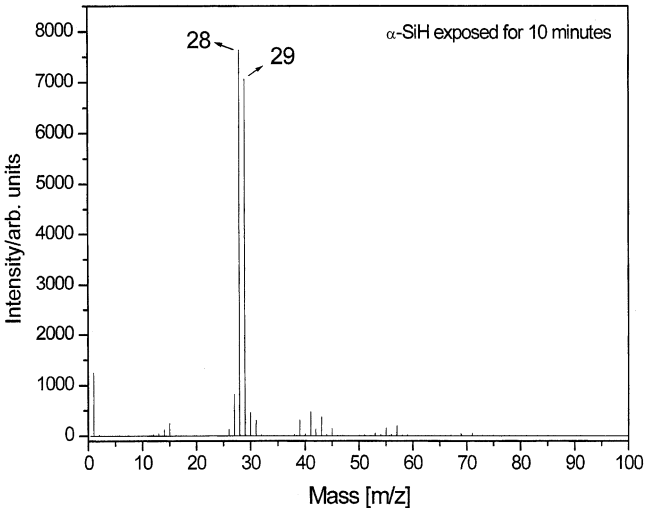

Fig. 3. The positive ion ToF-SIMS spectra ($m/e = 0-100$) of a nickel foil coated with an α-SiH film and exposed to air for 10 min that showed a large SiH^+ peak.

However, the contribution due to SiH^+ could be determined by calculating the ratio $R = {}^{28}Si/{}^{28}SiH + {}^{29}Si$. For comparison, the theoretical ratio of ${}^{28}Si/{}^{29}Si$ based on isotopic abundance is 19.6. R for the clean noncoated silicon wafer was 8.1. Whereas, R for the α-SiH sample was 1.15 indicating that the $m/z = 29$ peak was overwhelmingly due to SiH^+. Additional positive ion peaks of minority species are identified in Table 1.

The positive spectrum ($m/e = 0-100$) of a nickel foil coated with an α-SiH film and exposed to air for 10 days before the ToF-SIMS analysis is shown in Fig. 4. In this case R was 1.75 demonstrating that the sample was extraordinarily stable to air exposure. In contrast, R was 2.45 in the positive spectrum ($m/e = 0-100$) of the HF cleaned silicon wafer exposed to air for only 10 min before ToF-SIMS analysis as shown in Fig. 5.

ToF-SIMS is not directly quantitative for the stoichiometry of silicon hydrides. However, based on the isotopic abundance ratio ${}^{29}Si/{}^{28}Si$ of (0.051), the ${}^{28}SiH/{}^{28}Si$ ratio can be estimated. The ToF-SIMS determined ${}^{28}SiH/{}^{28}Si$ ratio for the HF-etched Si(1 1 1) surface and the α-SiH investigated was 0.35 and 0.82, respectively. It is generally recognized that each Si atom of the top layer of an HF-etched Si(1 1 1) surface is terminated by one H atom, i.e., the stoichiometry of the top layer is H–Si(1 1 1) [34]. Since ToF-SIMS measures the species mainly from the top layer, the maximum ${}^{28}SiH/{}^{28}Si$ ratio of an HF-etched Si(1 1 1) surface is unity. But, fragmentation of SiH into Si and H occurs during ToF-SIMS analysis due to the ionization processes caused by the bombardment with a Ga^+ source. Therefore, the ${}^{28}SiH/{}^{28}Si$ ratio from HF-etched Si(1 1 1) surfaces was observed to be far less than 1, but it was quantifiable and reproducible. Furthermore, the ${}^{28}SiH/{}^{28}Si$ ratio of the α-SiH investigated was about 2.3 times higher than that of the HF-etched Si(1 1 1).

Table 1
Summary of peaks from the positive spectra of Figs. 2–5

Nominal mass, *m/z*	Compound or fragment
1	H
6	Li
7	Li
12	C
13	CH
14	CH_2
15	CH_3
23	Na
24	C_2
26	C_2H_2
27	Al
27	C_2H_3
28	^{28}Si
29	^{29}Si
30	^{30}Si
31	$^{28}SiH_3$, $^{29}SiH_2$, ^{30}SiH, etc.
39	K
39	C_3H_3
40	Ca, SiC
40	C_3H_4
41	^{41}K
41	C_3H_5
42	SiN
43	SiNH, C_3H_7
44	SiO
45	SiOH
52	Cr, SiC_2
55	C_3H_7
56	Si_2
57	C_3H_9
69	^{69}Ga
71	C_5H_{11}
85	^{85}Rb
87	^{87}Rb

Given the H–Si(1 1 1) stoichiometry of HF-etched Si(1 1 1), it can be inferred that the average stoichiometry of the α-SiH investigated was $SiH_{2.3}$.

The negative ion spectra ($m/e = 0-100$) of the noncoated cleaned commercial silicon wafer and a nickel foil coated with an α-SiH film and exposed to air for 10 min before ToF-SIMS analysis are shown in Figs. 6 and 7, respectively. The control spectrum was dominated by oxide (O^- $m/z = 16$) and hydroxide (OH^- $m/z = 17$); whereas, spectrum of the α-SiH film was dominated by hydride ion (H^- $m/z = 1$). Very little oxide or hydroxide was observed. Additional negative ion peaks of minority species are identified in Table 2.

The negative spectrum ($m/e = 0-100$) of a nickel foil coated with an α-SiH film and exposed to air for 10 days before the ToF-SIMS analysis is shown in Fig. 8. In

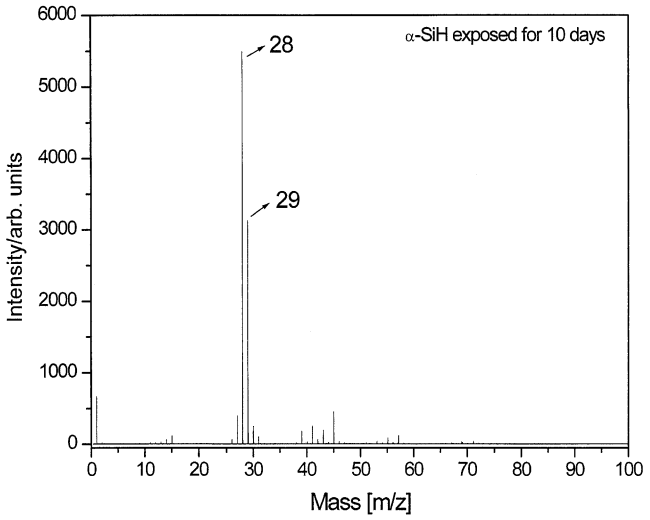

Fig. 4. The positive ion ToF-SIMS spectrum ($m/e = 0-100$) of a nickel foil coated with an α-SiH film and exposed to atmosphere for 10 days before the ToF-SIMS analysis that retained a large SiH^+ peak.

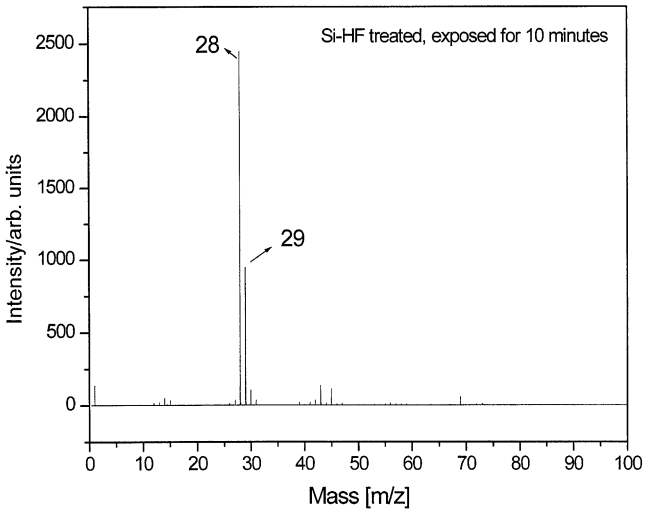

Fig. 5. The positive ion ToF-SIMS spectrum ($m/e = 0-100$) of the HF cleaned silicon wafer exposed to air for 10 min before ToF-SIMS analysis.

this case, hydride ion also dominated the negative spectrum demonstrating extraordinary air stability of the α-SiH film. The negative spectrum ($m/e = 0-100$) of the HF cleaned silicon wafer exposed to air for only 10 min before ToF-SIMS analysis is shown in Fig. 9, it also shows a dominant hydride as well as oxide, hydroxide, and some fluoride (F^- $m/z = 19$). However, the HF treated surface was not stable with prolonged air exposure. A dominant oxide peak was

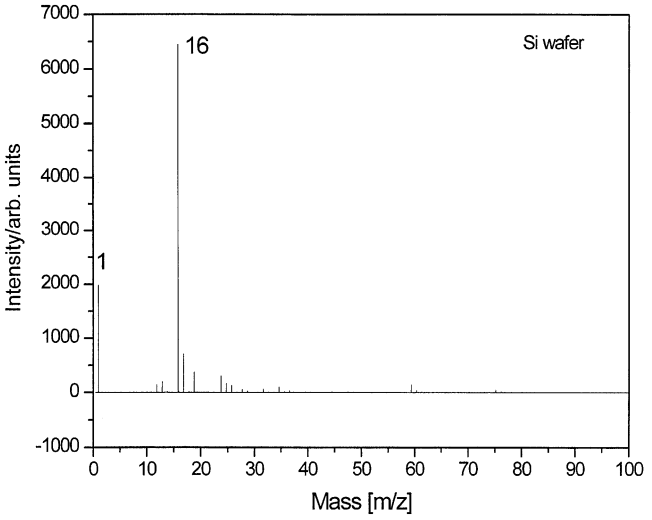

Fig. 6. The negative ion ToF-SIMS spectrum ($m/e = 0-100$) of the noncoated cleaned commercial silicon wafer (Alfa Aesar 99.99%).

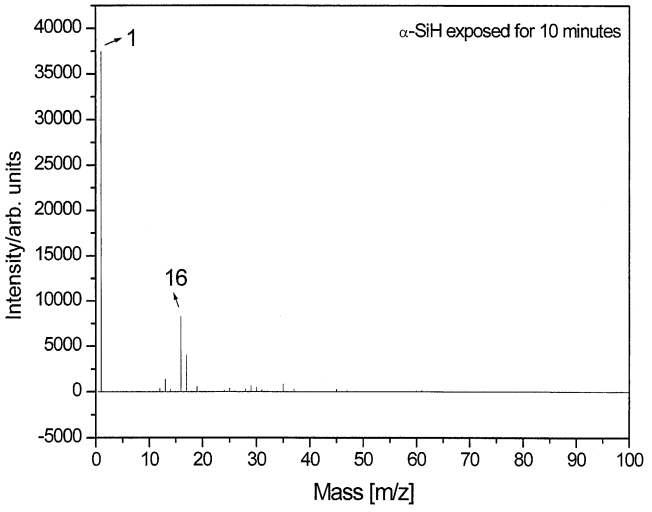

Fig. 7. The negative ion ToF-SIMS spectrum ($m/e = 0-100$) of a nickel foil coated with an α-SiH film and exposed to air for 10 min before ToF-SIMS analysis that was dominated by hydride ion.

observed in the negative spectrum ($m/e = 0-100$) of the HF cleaned silicon wafer exposed to air for only 3 h before ToF-SIMS analysis as shown in Fig. 10. Hydride was also observed in lesser amounts and may have resulted as a fragment of the observed hydroxide. Fluoride (F^- $m/z = 19$) was also observed. The ToF-SIMS

Table 2
Summary of peaks from the negative spectra of Figs. 6–10

Nominal mass, *m/z*	Compound or fragment
1	H
12	C
13	CH
14	CH_2
16	O
17	OH
18	H_2O
19	F
24	C_2
25	C_2H
26	C_2H_2
28	^{28}Si
29	^{29}Si
31	^{30}SiH, $^{29}SiH_2$, $^{28}SiH_3$
32	O_2, $^{28}SiH_4$
33	HO_2
35	^{35}Cl
37	^{37}Cl
40	^{28}SiC
41	^{29}SiC
42	^{30}SiC
44	^{28}SiO
45	$^{28}SiOH$
60	$^{29}SiO_2$
61	$^{29}SiO_2$, $^{28}SiO_2H$
62	$^{28}SiO_2H_2$, $^{29}SiO_2H$
75	SiO_2NH
76	$^{28}SiO_3$
77	$^{29}SiO_3$, $^{28}SiO_3H$

results from the HF treated surface is consistent with predominantly H termination of silicon dangling bonds as reported previously [3–5] that has undergone rapid oxidation to form mixed oxides such as SiOH.

These results indicate that the plasma reaction formed a highly stable hydrogenated silicon coating in the absence of fluorine observed on the HF treated surface. Remarkably, the α-SiH film was stable even after 10 days; whereas, the HF treated surface showed signs of oxidation over a 1500 times shorter time scale—10 min. At 3 h the HF treated surface had similarities to the control untreated silicon wafer which comprised a full oxide coating.

The plasma-reaction-formed α-SiH is proposed to comprise a more stable hydride ion than the H terminated silicon from HF treatment. Thus, the ion production efficiencies in ToF-SIMS analysis could be different making a comparison only qualitative and indicative of relative changes that occurred with timed air exposure. Since the Si 2p electron of all samples was equivalent except for energy shifts due to

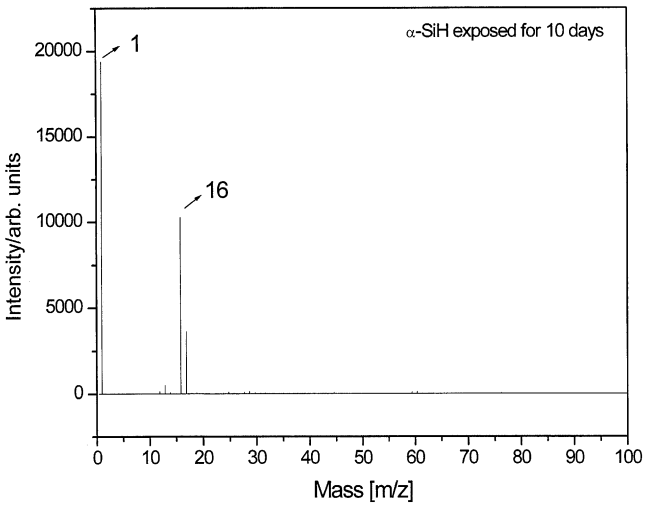

Fig. 8. The negative ion ToF-SIMS spectrum ($m/e = 0-100$) of a nickel foil coated with an α-SiH film and exposed to air for 10 days before the ToF-SIMS analysis that retained the dominant hydride ion peak.

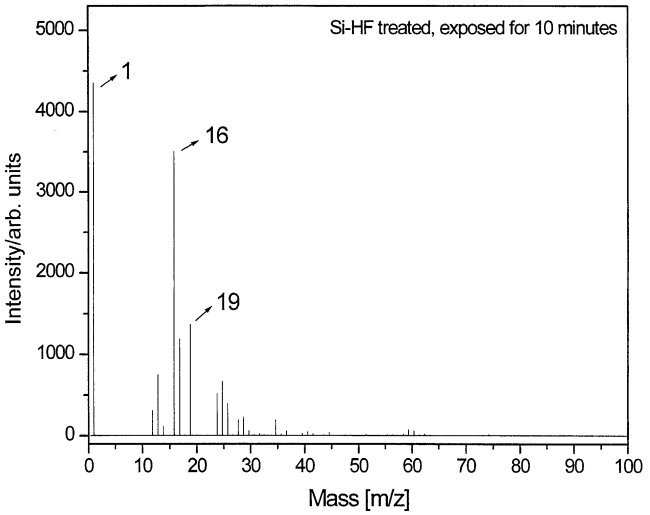

Fig. 9. The negative ion ToF-SIMS spectrum ($m/e = 0-100$) of the HF cleaned silicon wafer exposed to air for 10 min before ToF-SIMS analysis.

the presence of ordinary or novel hydride, or oxide, qualitative analysis was possible as given in the XPS section. As shown in this section, the ToF-SIMS results were confirmed by XPS.

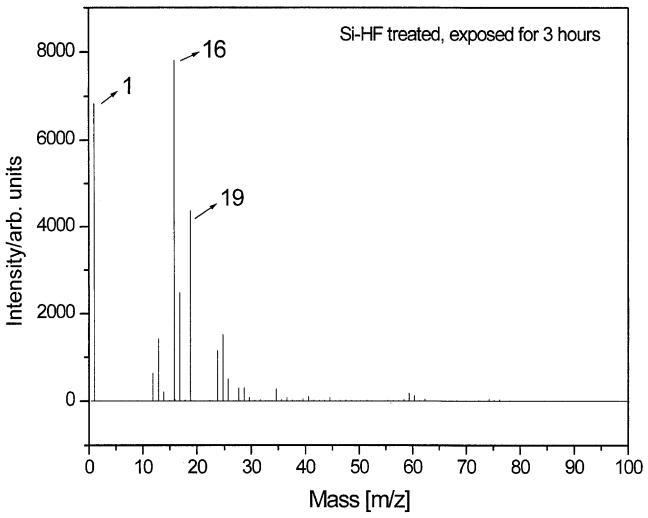

Fig. 10. The negative ion ToF-SIMS spectrum ($m/e = 0-100$) of the HF cleaned silicon wafer exposed to air for 3 h before ToF-SIMS analysis showing a dominant oxide peak.

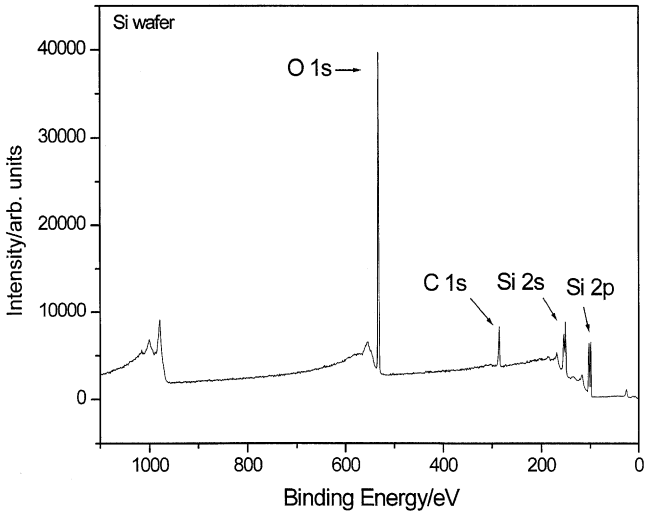

Fig. 11. The XPS survey scan of the noncoated cleaned commercial silicon wafer showing a large amount of oxide and carbon contamination of the surface.

3.2. XPS

The XPS survey spectra of the noncoated cleaned commercial silicon wafer (control) and a nickel foil coated with an α-SiH film and exposed to air for 20 min were obtained over the region $E_b = 0-1200$ eV and are shown in Figs. 11 and 12, respectively. The survey spectra permitted the determination of all of the elements

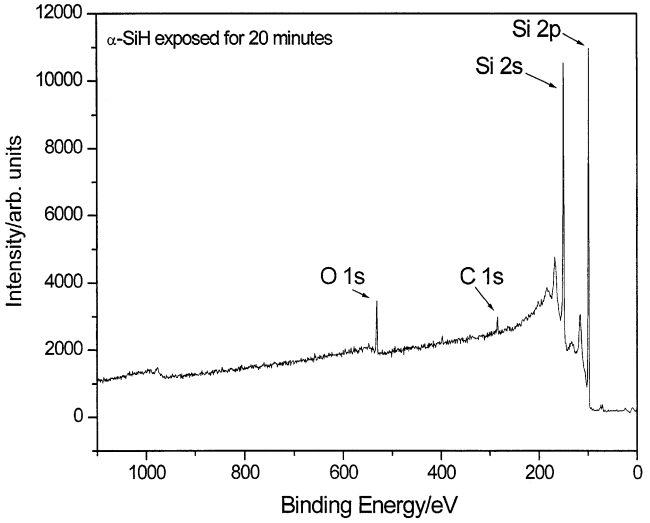

Fig. 12. The XPS survey scan of a nickel foil coated with an α-SiH film and exposed to air for 20 min before XPS analysis showing minimal oxide and carbon.

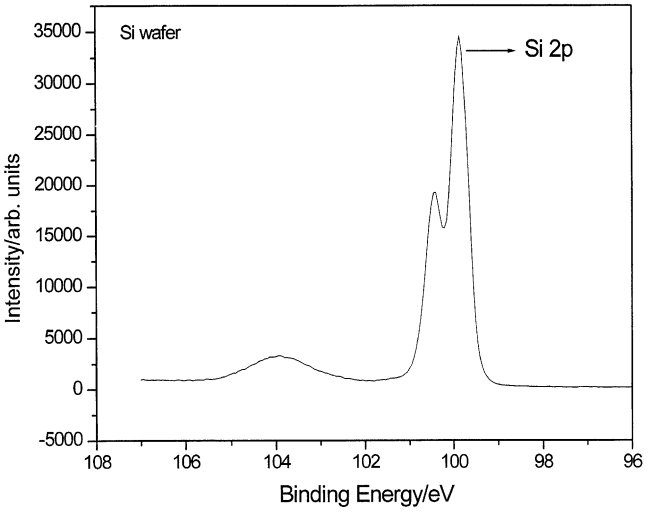

Fig. 13. The XPS spectrum (96–108 eV) in the region of the Si 2p peak of the noncoated cleaned commercial silicon wafer showing a large SiO_2 in the region of 104 eV.

present and detected shifts in the binding energies of the Si 2p peak, which also identifies the presence or absence of SiO_2. The major species identified in the XPS spectrum of the control sample were silicon, oxygen, and carbon. The α-SiH sample contained essentially silicon with negligible oxygen and carbon.

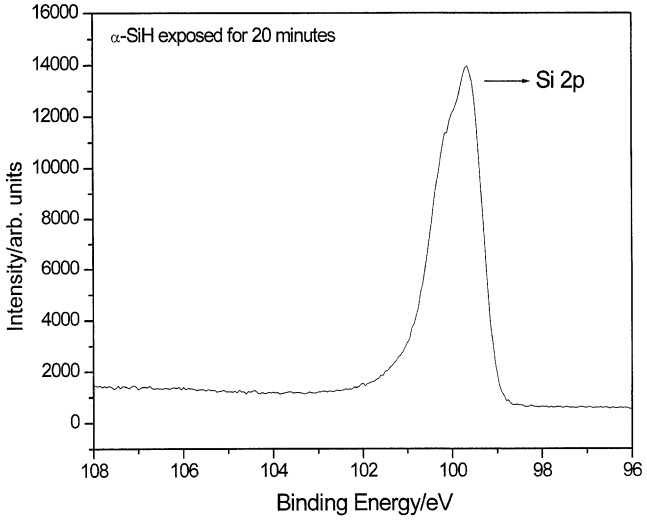

Fig. 14. The XPS spectrum (96–108 eV) in the region of the Si 2p peak of a nickel foil with an α-SiH film and exposed to air for 20 min before XPS analysis showing no oxide in the region of 104 eV.

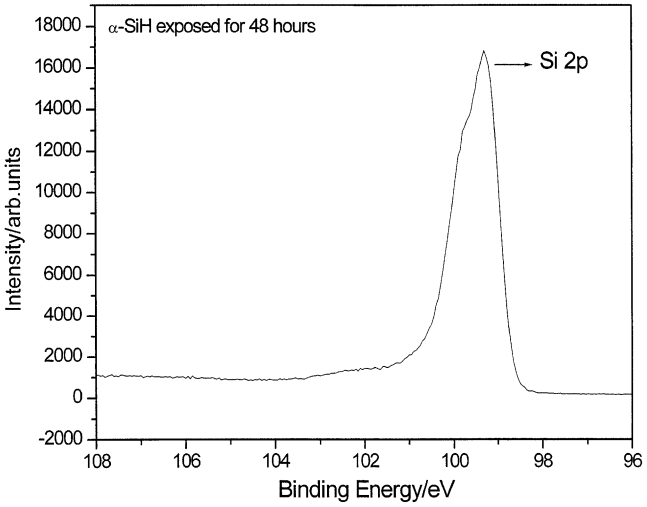

Fig. 15. The XPS spectrum (96–108 eV) in the region of the Si 2p peak of a nickel foil coated with an α-SiH film and exposed to air for 48 h before the XPS analysis showing no oxide at 104 eV and possibly trace SiOH in the region of 102 eV.

The XPS spectra (96–108 eV) in the region of the Si 2p peak of the noncoated cleaned commercial silicon wafer and a nickel foil coated with an α-SiH film and exposed to air for 20 min are shown in Figs. 13 and 14, respectively. The XPS spectrum of the control silicon wafer shows a large SiO_2 content at 104 eV as given by Wagner et al. [35]. In contrast, the α-SiH sample had essentially no SiO_2. In

addition, spin–orbital coupling gives rise to a split Si 2p peak in pure silicon, but this peak changed to a single broad peak upon reaction to form the α-SiH film indicative of amorphous silicon.

The XPS spectrum (96–108 eV) in the region of the Si 2p peak of a nickel foil coated with an α-SiH film and exposed to air for 48 h before the XPS analysis is shown in Fig. 15. Essentially no SiO_2 was observed at 104 eV demonstrating that the sample was extraordinarily stable to air exposure. Perhaps trace SiOH is present in the region of 102 eV potentially due to less than 100% coverage of the surface with the α-SiH film; rather, some silicon deposition may have occurred. In contrast, the XPS spectrum (96–108 eV) in the region of the Si 2p peak of the HF cleaned silicon wafer exposed to air for 10 min before XPS analysis was essentially fully covered by partial oxides SiO_x such as SiOH. The mixed silicon oxide peak in the region of 101.5–104 eV shown in Fig. 16 was essentially the same percentage of the Si 2p as that of the SiO_2 peak of the uncleaned wafer shown at 104 eV in Fig. 13. In addition, the O ls peak of the α-SiH film exposed to air for 48 h shown in Fig. 17 was negligible; whereas, that of the HF cleaned wafer exposed to air for 10 min was intense as shown in Fig. 18.

The 0–70 eV and the 0–85 eV binding energy region of high resolution XPS spectra of the commercial silicon wafer and a HF cleaned silicon wafer exposed to air for 10 min before XPS analysis are shown in Figs. 19 and 20, respectively. Only a large O 2s peak in the low binding energy region was observed in each case. In Fig. 19, the C, O, and Si valance bands are observed in the region 0–10 eV. The 0–70 eV binding energy region of a nickel foil coated with an α-SiH film and exposed to air for 20 min before XPS analysis is shown in Fig. 21. By comparison of the α-SiH sample to the controls, novel XPS peaks were identified at 11, 43, and 55 eV. These peaks do not

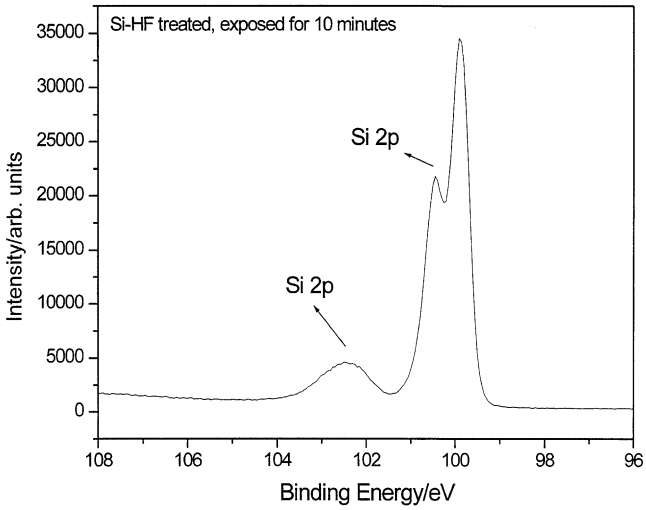

Fig. 16. The XPS spectrum (96–108 eV) in the region of the Si 2p peak of the HF cleaned silicon wafer exposed to air for 10 min before XPS analysis showing a very large SiO_x peak in the region of 101.5–104 eV.

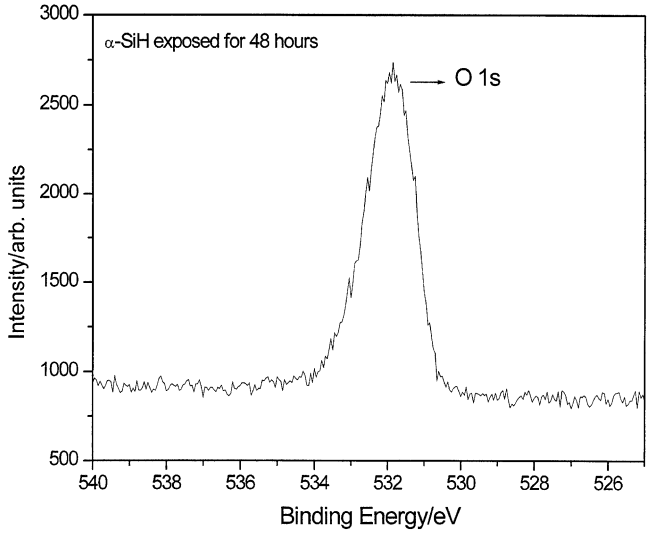

Fig. 17. The XPS spectrum (525–540 eV) in the region of the O 1s peak of a nickel foil coated with an α-SiH film and exposed to air for 48 h before XPS analysis showing a minimal amount of oxide.

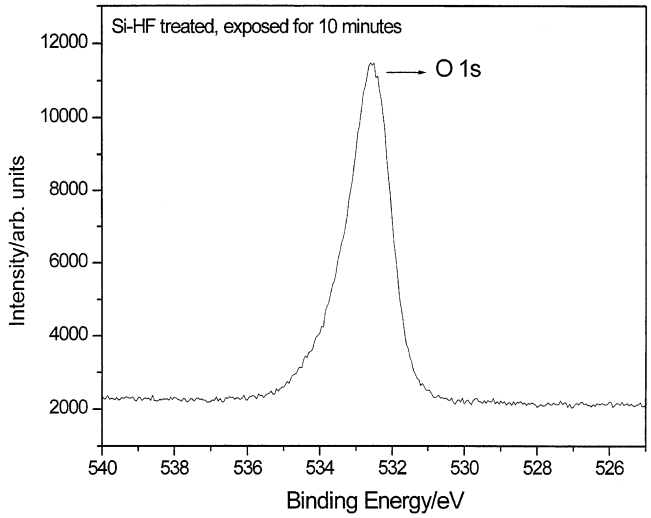

Fig. 18. The XPS spectrum (525–540 eV) in the region of the O 1s peak of the HF cleaned silicon wafer exposed to air for 10 min before XPS analysis showing a very large oxide peak.

correspond to any of the primary elements, silicon, carbon, or oxygen, shown in the survey scan in Fig. 12, wherein the peaks of these elements are given by Wagner et al. [35]. Hydrogen is the only element which does not have primary element peaks; thus, it is the only candidate to produce the novel peaks and correspond to the H content of the SiH coatings. These peaks closely matched hydrides formed by the catalytic

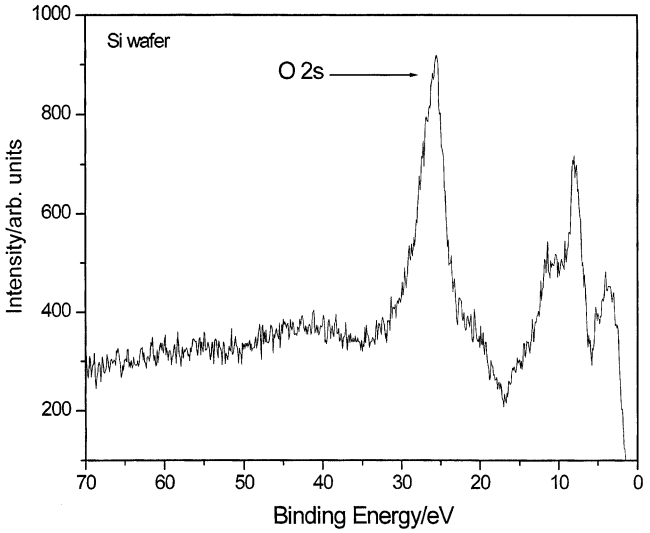

Fig. 19. The 0–70 eV binding energy region of a high resolution XPS spectrum of the commercial silicon wafer showing only a large O 2s peak in the low binding energy region.

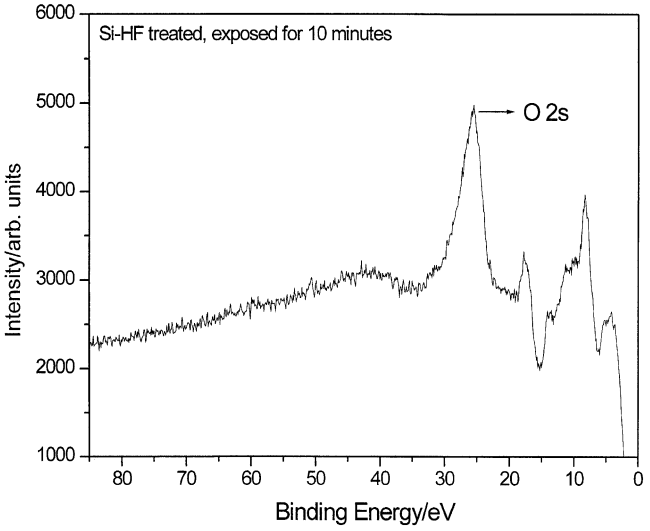

Fig. 20. The 0–85 eV binding energy region of a high resolution XPS spectrum of the HF cleaned silicon wafer exposed to air for 10 min before XPS analysis showing only a large O 2s peak in the low binding energy region.

reaction of He^+ with atomic hydrogen and subsequent reactions to form highly stable silicon hydride products α-SiH that were discussed previously [31].

These results indicate that the plasma reaction formed a highly stable novel hydrogenated coating; whereas, the control comprised an oxide coating or an

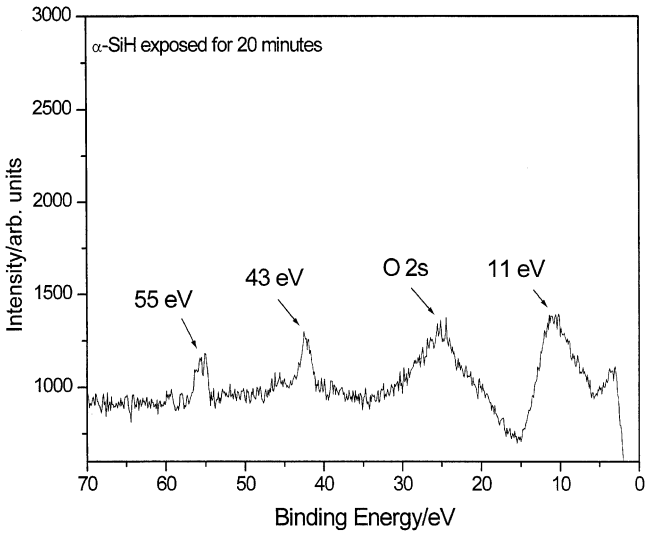

Fig. 21. The 0–70 eV binding energy region of a high-resolution XPS spectrum of a nickel foil coated with an α-SiH film and exposed to air for 20 min before XPS analysis. The novel peaks observed at 11, 43 and 55 eV which could not be assigned to the elements identified by their primary XPS peaks matched and were assigned to highly stable silicon hydrides formed by the catalytic reaction of He^+ and atomic hydrogen.

unstable hydrogen terminated silicon surface which rapidly formed an oxide passivation layer. The hydrogen content of the α-SiH coating appears to be novel silicon hydrides with high binding energies which account for the exceptional air stability.

4. Conclusions

Nickel substrates were coated by the reaction product of a low-pressure microwave discharge plasma of SiH_4 (2.5%)/He (96.6%)/H_2 (0.9%). The ToF-SIMS identified the coatings as hydride by the large SiH^+ peak in the positive spectrum and the dominant H^- in the negative spectrum. XPS identified the H content of the SiH coatings as hydride corresponding to peaks at 11, 43, and 55 eV, respectively, in the absence of any other identifiable primary element peaks. The novel hydrides are proposed to form by the catalytic reaction of He^+ with atomic hydrogen with subsequent reactions to form highly stable silicon hydride products. The SiH coating was amorphous as indicated by the shape of the Si 2p peak and was remarkably stable to air exposure. After a 48 h exposure to air, essentially no oxygen was observed as evidence by the negligible O 1s peak at 531 eV and absence of any SiO_x Si 2p peak in the region of 102–104 eV. The highly stable amorphous silicon hydride coating may advance the production of integrated circuits and microdevices by resisting the oxygen passivation of the surface and possibly altering the dielectric constant and band gap to increase device performance.

References

[1] W. Kern, Semicond. Int. 7 (4) (1984) 94.
[2] F.J. Grunthaner, P.J. Grunthaner, Mater. Sci. Rep. 1 (1986) 69.
[3] M. Grudner, H. Jacob, Appl. Phys. A 39 (1986) 73.
[4] H. Ubara, T. Imura, A. Hiraki, Solid State Commun. 50 (1984) 673.
[5] E. Yablonovitch, D.L. Allara, C.C. Chang, T. Gmitter, T.B. Bright, Phys. Rev. Lett. 57 (1986) 249.
[6] R.A. Street, Hydrogenated Amorphous Silicon, Cambridge University Press, Cambridge, 1991, pp. 18–61.
[7] M.A. Green, Photovoltaics: technology overview, Energy Policy 28 (2000) 989–998.
[8] R. Mills, M. Nansteel, P. Ray, Argon–hydrogen–strontium discharge light source, IEEE Trans. Plasma Sci. 30 (2) (2002) 639–653.
[9] R. Mills, B. Dhandapani, M. Nansteel, J. He, A. Voigt, Identification of compounds containing novel hydride ions by nuclear magnetic resonance spectroscopy, Int. J. Hydrogen Energy 26 (9) (2001) 965–979.
[10] R. Mills, P. Ray, Spectral emission of fractional quantum energy levels of atomic hydrogen from a helium–hydrogen plasma and the implications for dark matter, Int. J. Hydrogen Energy 27(3) 301–322.
[11] R.L. Mills, P. Ray, B. Dhandapani, J. He, Extreme ultraviolet spectroscopy of helium-hydrogen plasma, J. Phys. D.: Appl. Phys. 36 (2003) 1535–1542.
[12] R.L. Mills, P. Ray, B. Dhandapani, M. Nansteel, X. Chen, J. He, New power source from fractional quantum energy levels of atomic hydrogen that surpasses internal combustion, J. Mol. Struct. 643 (1–3) (2002) 43–54.
[13] R. Mills, J. Dong, Y. Lu, Observation of extreme ultraviolet hydrogen emission from incandescently heated hydrogen gas with certain catalysts, Int. J. Hydrogen Energy 25 (2000) 919–943.
[14] R.L. Mills, P. Ray, A comprehensive study of spectra of the bound-free hyperfine levels of novel hydride ion $He^{-}(1/2)$, hydrogen, nitrogen and air, Int. J. Hydrogen Energy 28 (8) (2003) 825–871.
[15] R. Mills, Spectroscopic identification of a novel catalytic reaction of atomic hydrogen and the hydride ion product, Int. J. Hydrogen Energy 26 (10) (2001) 1041–1058.
[16] R. Mills, P. Ray, Spectroscopic identification of a novel catalytic reaction of potassium and atomic hydrogen and the hydride ion product, Int. J. Hydrogen Energy 27 (2) (2002) 183–192.
[17] R.L. Mills, P. Ray, Spectroscopic identification of a novel catalytic reaction of rubidium ion with atomic hydrogen and the hydride ion product, Int. J. Hydrogen Energy 27 (9) (2002) 927–935.
[18] R. Mills, P. Ray, Vibrational spectral emission of fractional-principal-quantum-energy-level hydrogen molecular ion, Int. J. Hydrogen Energy 27 (5) (2002) 533–564.
[19] R.L. Mills, P. Ray, J. Dong, M. Nansteel, B. Dhandapani, J. He, Spectral emission of fractional-principal-quantum-energy-level atomic and molecular hydrogen, Vib. Spectrosc. 31 (2) (2003) 195–213.
[20] H. Conrads, R. Mills, Th. Wrubel, Emission in the deep vacuum ultraviolet from a plasma formed by incandescently heating hydrogen gas with trace amounts of potassium carbonate, Plasma Sources Sci. Technol. 12 (2003) 389–395.
[21] R. Mills, T. Onuma, Y. Lu, Formation of a hydrogen plasma from an incandescently heated hydrogen-catalyst gas mixture with an anomalous afterglow duration, Int. J. Hydrogen Energy 26 (7) (2001) 749–762.
[22] R.L. Mills, P. Ray, B. Dhandapani, J. He, Comparison of excessive Balmer α line broadening of glow discharge and microwave hydrogen plasmas with certain catalysts, J. Appl. Phys. 92 (12) (2002) 7008–7022.
[23] R.L. Mills, P. Ray, Substantial changes in the characteristics of a microwave plasma due to combining argon and hydrogen, New J. Phys. 4 (2002) 22.1–22.17, www.njp.org.
[24] R.L. Mills, X. Chen, P. Ray, J. He, B. Dhandapani, Plasma power source based on a catalytic reaction of atomic hydrogen measured by water bath calorimetry, Thermochim. Acta, http://dx.doi.org/10.1016/S0040-6031(03)00228-4, in press.

[25] R.L. Mills, P. Ray, B. Dhandapani, J. He, Emission spectroscopic identification of fractional Rydberg states of atomic hydrogen formed by a catalytic helium–hydrogen plasma reaction, Vacuum, submitted for publication.
[26] R. Mills, P. Ray, R.M. Mayo, The potential for a hydrogen water-plasma laser, Appl. Phys. Lett. 82 (11) (2003) 1679–1681.
[27] R.L. Mills, P. Ray, E. Dayalan, B. Dhandapani, J. He, Comparison of excessive Balmer α line broadening of inductively and capacitively coupled RF, microwave, and glow discharge hydrogen plasmas with certain catalysts, IEEE Trans. Plasma Sci. 31 (3) (2003) 338–355.
[28] R. Mills, B. Dhandapani, M. Nansteel, J. He, T. Shannon, A. Echezuria, Synthesis and characterization of novel hydride compounds, Int. J. Hydrogen Energy 26 (4) (2001) 339–367.
[29] R. Mills, B. Dhandapani, N. Greenig, J. He, Synthesis and characterization of potassium iodo hydride, Int. J. Hydrogen Energy 25 (12) (2000) 1185–1203.
[30] R. Mills, E. Dayalan, P. Ray, B. Dhandapani, J. He, Highly stable novel inorganic hydrides from aqueous electrolysis and plasma electrolysis, Electrochim. Acta 47 (24) (2002) 3909–3926.
[31] R.L. Mills, B. Dhandapani, J. He, Synthesis and characterization of a highly stable amorphous silicon hydride, Int. J. Hydrogen Energy, in press.
[32] B. Sefsaf, B. Carriere, J.P. Deville, Electron-beam induced growth of ultrathin oxide-films on Si(1 0 0) surfaces, Microsci. Microanal. Microstruct. 3 (1) (1992) 15–22.
[33] PHI Trift II, ToF-SIMS Technical Brochure, Eden Prairie, MN 55344, 1999.
[34] G.S. Higashi, Y.J. Chabal, G.W. Trucks, K. Raghavachari, Appl. Phys. Lett. 56 (1990) 656.
[35] C.D. Wagner, W.M. Riggs, L.E. Davis, J.F. Moulder, G. E. Mulilenberg (Eds.), Handbook of X-ray Photoelectron Spectroscopy, Perkin-Elmer Corp., Eden Prairie, MN, 1997.